DESIGN AND APPLICATION OF A NEW PLANAR BALUN

Younes Mohamed

Thesis Prepared for the Degree of

MASTER OF SCIENCE

UNIVERSITY OF NORTH TEXAS

May 2014

APPROVED:

Shengli Fu, Major Professor and Interim Chair of the Department of Electrical Engineering
Hualiang Zhang, Co-Major Professor
Hyoung Soo Kim, Committee Member
Costas Tsatsoulis, Dean of the College of Engineering
Mark Wardell, Dean of the Toulouse Graduate School

Mohamed, Younes. *Design and Application of a New Planar Balun*. Master of Science (Electrical Engineering), May 2014, 41 pp., 2 tables, 29 figures, references, 21 titles.

The baluns are the key components in balanced circuits such balanced mixers, frequency multipliers, push–pull amplifiers, and antennas. Most of these applications have become more integrated which demands the baluns to be in compact size and low cost. In this thesis, a new approach about the design of planar balun is presented where the 4-port symmetrical network with one port terminated by open circuit is first analyzed by using even- and odd-mode excitations. With full design equations, the proposed balun presents perfect balanced output and good input matching and the measurement results make a good agreement with the simulations. Second, Yagi-Uda antenna is also introduced as an entry to fully understand the quasi-Yagi antenna. Both of the antennas have the same design requirements and present the radiation properties. The arrangement of the antenna's elements and the end-fire radiation property of the antenna have been presented. Finally, the quasi-Yagi antenna is used as an application of the balun where the proposed balun is employed to feed a quasi-Yagi antenna. The antenna is working in the S-band radio frequency and achieves a measured 36% fractional bandwidth for return loss less than -10 dB. The antenna demonstrates a good agreement between its measurement and simulation results. The impact of the parasitic director on the antenna's performance is also investigated. The gain and the frequency range of the antenna have been reduced due to the absence of this element. This reduction presents in simulation and measurement results with very close agreement.

ACKNOWLEDGEMENTS

I would like to thank Allah. I would like to express my sincere gratitude to my advisor Dr. Shengli Fu, who has the attitude and the substance of a genius: he motivated me with his knowledge, provide me invaluable insights, and guided me to set a goal in my professional life.

I would like to express my deepest appreciation to my co-advisor Dr. Hualiang Zhang, who has conveyed a spirit of adventure in regard to thought, teaching, and research. His expertise in RF and microwave field has improved my research skills and prepared me for future challenges. My completion of this thesis could not have been accomplished without the invaluable support and guidance of Dr. Zhang.

I would like to thank Dr. Hyoung Soo Kim for his support and encouragement as committee member of my thesis and all of my lab mates for their help and cooperation.

Finally, I would also like to extend my deepest gratitude to my parents and my wife for their constant source of inspiration and support.

TABLE OF CONTENTS

Page

LIST OF TABLES

Page

LIST OF FIGURES

Page

CHAPTER 1

INTRODUCTION

1.1 Motivation

Since Nathan Marchand, who firstly proposed the balun in 1944, various balun configurations have been reported for applications in microwave integrated circuits (MICs) and monolithic microwave integrated circuits (MMICs). The design of many symmetric microwave structures, such as mixers, balanced amplifiers, and antennas require a balanced feed in order to work properly. Coaxial cables are often used to guide signals at RF and microwave frequencies. However, these cables are unbalanced structures, and therefore cannot provide a balanced feed if they are connected directly to symmetric microwave circuits. In order to properly transition between balanced and unbalanced structures, a balun (balanced -to- unbalanced) is required.

1.2 Contribution of Thesis

In general, balun is a circuit that transforms unbalanced signals to balanced signals or versa vice. This thesis introduces a novel distributed balun, including full design equations. From 4-port network with open circuit at port 4 this new balun is designed. It presents a transmission stop in even-mode circuit to achieve perfect amplitude and phase balance at the balun output and provides odd-mode impedance to be twice of input impedance in odd-mode circuit to achieve a perfect matching at the balun input. This novel balun is employed to feed quasi-Yagi antenna.

1.3 Overview of Thesis

This thesis presents a new approach about the design of planar balun and employs the proposed balun to feed a quasi-Yagi antenna.

The second chapter introduces a novel distributed balun and presents the fundamental design equations. The proposed structure is based on a symmetrical 4-port network where the port four is terminated with an open circuit. To achieve a transmission stop in the short circuit case, an open-ended stub is added to the port one side. In open circuit case, the equivalent ABCD matrix of the transmission lines is set to be equal the ABCD matrix of λ/4 impedance transformer in order to achieve good input matching. Finally, to verify the design concept, a microstrip balun operating at 2.4 GHz is simulated using Hyperlynx 3D and fabricated on Roger RO4003 printed circuit board. Measurement results are in good agreement with the simulation procedures.

In the third chapter, the principle of Yagi-Uda antenna is presented as an entry to understand the quasi-Yagi antenna since they have the same fundamental concept and design requirements. Yagi-Uda antenna as an end-fire array is discussed.

In the fourth chapter, to verify the performance of the proposed balun, a uniplanar quasi-Yagi antenna system is designed and fabricated on RO4003 printed circuit board. The antenna operates in the S-band portion of the microwave spectrum. The measurement results agree well with the design theory.

Finally, the last chapter concludes the thesis and outlines its achievement. Furthermore, direction for the future work is also presented.

CHAPTER 2

A NEW DISTRIBUTED BALUN

2.1 Introduction

With rapid development of wireless communication technologies, the demand on low profile and low-cost passive components is highly increased. One of these key components is a balun, which is an essential circuit element in balanced devices, such as double-balanced mixer, frequency multipliers, push-pull amplifiers, and antennas. The main function of the balun is to match an unbalanced circuit structure to a balanced circuit structure. The signals at the balanced circuit are equal in magnitude throughout the frequencies of interest with 180-degree phase difference. Impedance matching between an unbalance port and balanced ports is the other purpose of using the balun in RF and microwave circuits.

The balun configurations include lumped, distributed, or both lumped and distributed elements. The distributed baluns consist of N sections of transmission lines [5]-[7]. The simplest distributed balun is a half wavelength transmission line. In spite of its small size, this balun is an inherently narrow band device [6]. By increasing the number half wavelength transmission lines, the bandwidth of the balun can be increased [7]. However, this design will occupy a large area in microwave circuits. Parallel plate and coupled line baluns are also distributed baluns [8]-[10]. Some of these distributed-element baluns require nonplanar or multilayer structures that increase design complexity. The baluns can be also designed by using lumped elements. Lumped-element baluns that function as low-pass and high-pass filter structures are suited for low frequency and MMIC applications [11], [12]. The theory of lumped-

element baluns is based on the rat-race ring hybrid. The distributed transmission lines of the rat-race ring are replaced by lumped element equivalent circuits. The quarter wavelength lines of the rat-race ring are replaced by lumped element low-pass filter networks. The three quarter wavelength line is replaced by a high-pass filter network [6]. These baluns need many lumped components. The third balun configuration consists of both lumped and distributed elements and has been introduced in [13]-[15]. The derivations of these baluns relay on experimental methods, parametric analysis [15], or electromagnetic simulations [14].

The balun described in this chapter is a distributed-element balun, and its realization is based on even- and odd-mode analysis techniques for 3-port network. This approach provides valuable insight to the synthesis and design requirements of these balun structures by specifying the requirements of the odd and even mode parameters of the 4-port symmetrical networks. Development of new balun structures and exact design equations at the operating frequency of this class of baluns will be presented.

2.2 Theory and Analysis

The balun presented here is a three-port device realized and converted from a symmetrical four-port network where one of the ports is terminated with an open circuit, as shown in Fig. 2.1. The balun will convert an unbalanced input with source impedance Z_{in} into balanced outputs with load impedances Z_{out}.

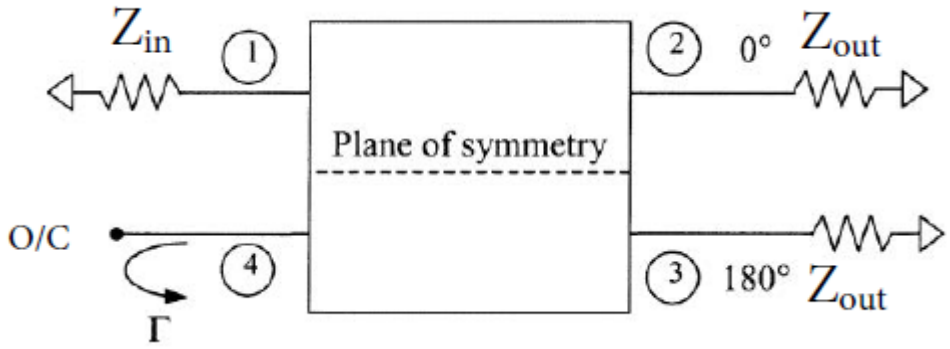

Fig. 2.1. A symmetrical four-port network with one port terminated in an open circuit.

The impedances Z_{in} and Z_{out} are equal. Thus, the balun does not perform impedance transformation between the source and the load. In order for the 3-port network to behave as a balun, the following conditions has to be satisfied

$$S_{21} = -S_{31} \tag{2.1}$$

$$S_{11} = 0 \tag{2.2}$$

To achieve perfect signals with equal amplitude and opposite phase at the balanced output ports ($S_{21} = -S_{31}$) and a good input matching ($S_{11} = 0$) at the balun input, the even-mode transmission coefficient T_{even} and the odd-mode impedance Z_{odd} should be obtained as

$$\mathrm{T}_{even} = 0 \tag{2.3}$$

$$\mathrm{Z}_{odd} = 2\,Z_0 \tag{2.4}$$

to realize the equations 2.3 and 2.4, even- and odd-mode analysis is employed on the schematic diagram of the balun shown in Fig. 2.2. The proposed balun consists of 2 sections of transmission lines of impedance Z_2 and electrical length θ_2 in series and 4 transmission lines of impedances Z_1 and Z_3 and electrical length θ_1 and θ_3 in parallel. At

the port one side, an open-ended transmission line of impedance $\frac{Z_1}{2}$ and electrical length $\left(\frac{\pi}{2}-\theta_1\right)$ connected in parallel with shunted lines at that port.

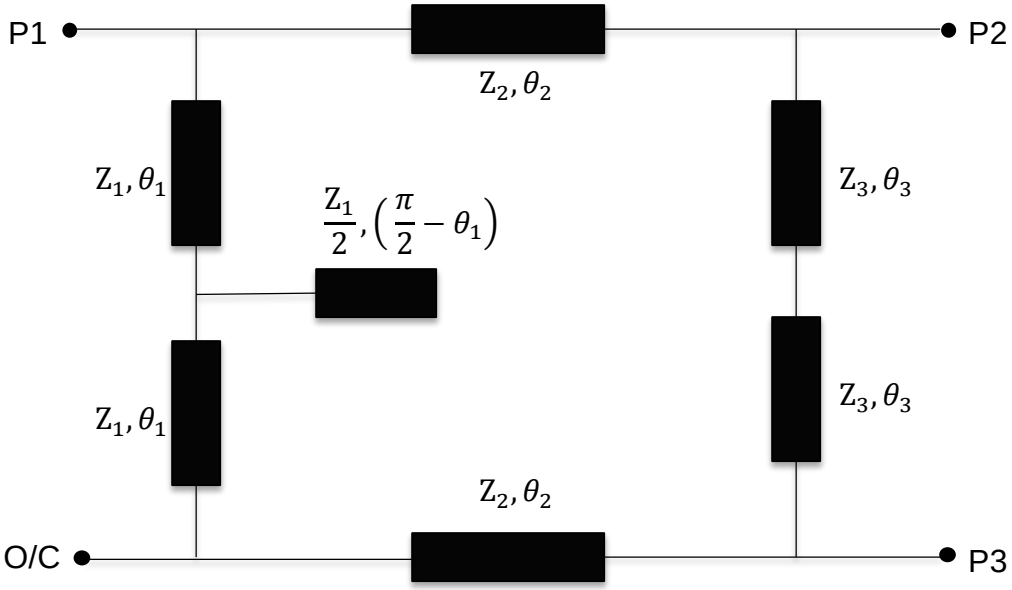

Fig. 2.2. Schematic diagram of the proposed three-port balun.

2.2.1 Even-Mode Excitation of Balun Circuit

The balun structure has even symmetry, and thus the plane of symmetry becomes a virtual open as illustrated in Fig. 2.3. The open-ended transmission line is divided into 2 sections of impedances Z_1 and electrical lengths $\left(\frac{\pi}{2}-\theta_1\right)$. At P1 the two transmission lines of impedance Z_1 and electrical lengths θ_1 and $\left(\frac{\pi}{2}-\theta_1\right)$ become one transmission line of impedance Z_1 and electrical length $\frac{\pi}{2}$. According to transmission line theory, the input impedance of terminated transmission line at the location of the generator,$z = -L$, the input impedance is:

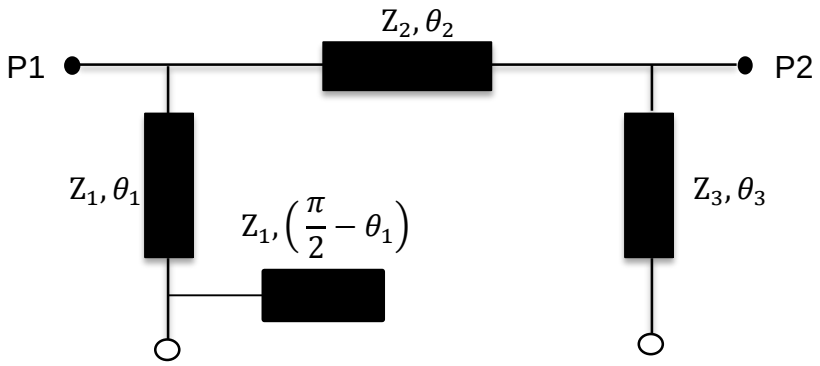

Fig. 2.3. Even-mode circuit of the proposed balun.

$$Z_{in} = Z_{(z=-L)} = Z_0 \frac{Z_L + Z_0 \tanh \gamma L}{Z_0 + Z_L \tanh \gamma L} \tag{2.5}$$

for a lossless transmission line, the input impedance becomes

$$Z_{in} = Z_0 \frac{Z_L + jZ_0 \tanh \beta L}{Z_0 + jZ_L \tanh \beta L} \tag{2.6}$$

a special case of input impedance of terminated transmission line when one of its terminals is open, the equation 2.6 can be reduced as

$$Z_{in}|_{Z_L \to \infty} = -jZ_0 \cot(\beta L) \tag{2.7}$$

the input impedance Z_{in} is purely reactive and depends on the length of the transmission line L

- If $L = \lambda/4, 3\lambda/4, \ldots, n\lambda/4, n = 1, 3, 5, ..$, the input impedance is zero, and the transmission line acts like a short circuit
- If $L = \lambda/2, \lambda, 3\lambda/2, \ldots, n\lambda/2, n = 1, 2, 3, ..$, the input impedance is infinite, and the transmission line acts like an open circuit

In the circuit shown in Fig. 2.4, the input impedance of the open-ended transmission line

at port one is zero since $\beta L = {}^{\pi}/_{2}$ in equation 2.7. This makes P1 connected to a short circuit and the input impedance Z_{in} of the corresponding even-mode half-circuit is zero, and consequently no power transmitted to P2 and the transmission coefficient T_{even} is zero.

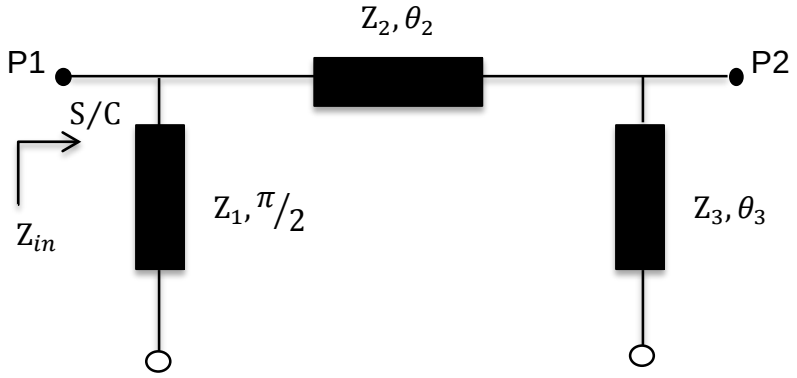

Fig. 2.4 Even-mode circuit with short circuit at P1

2.2.2 Odd-Mode Excitation of Balun Circuit

Since the balun circuit has odd symmetry, the plane of symmetry becomes a virtual short, and the corresponding odd-mode half-circuit of the balun is connected to the ground as shown in Fig. 2.5. The equation 2.4 shows that to achieve perfect matching at the balun input in the short-circuit case; the odd-mode impedance must be twice the characteristic impedance Z_0 of the odd-mode circuit. For simplicity the impedances and electrical lengths of two shunted transmission lines are assumed to be equals, and the three sections of transmission lines in Fig. 2.5 is treated as one transmission line of impedance $Z_0 = 70.7\,\Omega$ and electrical length $\theta = {}^{\pi}/_{2}$. This transmission line is commonly called quarter wavelength transmission line and preforms a transformation between the input and output impedances as follows:

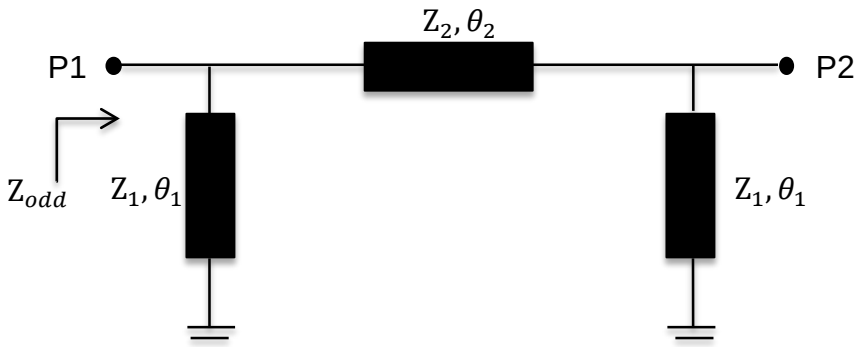

Fig. 2.4. Odd-mode circuit of the proposed balun.

$$Z_{in} = \frac{Z_0^2}{Z_L} \tag{2.8}$$

by using this expression, the odd-mode impedance will be

$$Z_{odd} = \frac{Z_T^2}{Z_L} \tag{2.9}$$

supposing that the equivalent transmission line of impedance Z_T and electrical length θ_T is equal to the quarter wavelength transmission line. Thus, the total of ABCD matrices of the three transmission lines of the odd-mode circuit should be equal to the ABCD matrix of the quarter wavelength line.

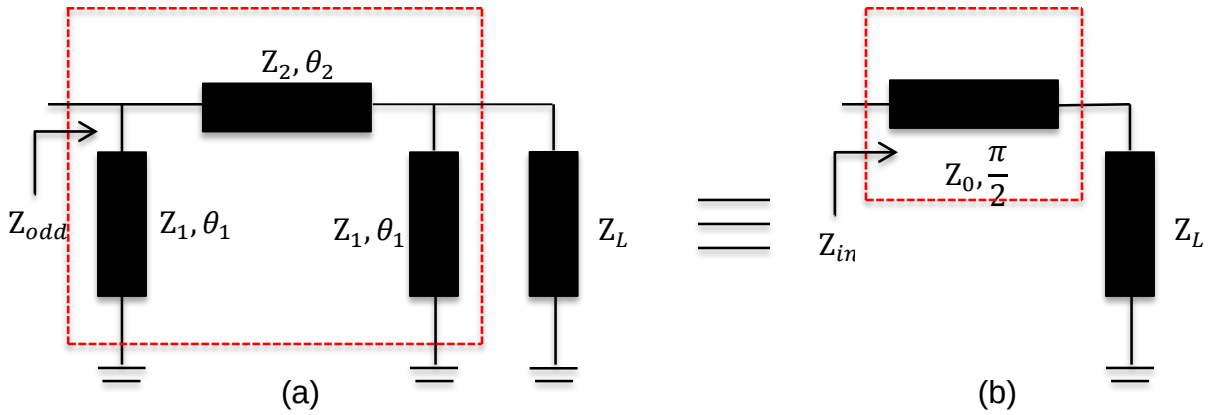

Fig. 2.5. (a) The odd-mode circuit of the proposed balun, (b) the equivalent circuit of the odd-mode circuit.

ABCD matrix of two shunt transmission lines is

$$\begin{bmatrix} 1 & 0 \\ -j\,\frac{1}{Z_1 \tan\theta_1} & 1 \end{bmatrix} \tag{2.10}$$

ABCD matrix of series transmission line is

$$\begin{bmatrix} \cos\theta_2 & j\,Z_2\ \sin\theta_2 \\ j\,\frac{1}{Z_2}\sin\theta_2 & \cos\theta_2 \end{bmatrix} \tag{2.11}$$

the total ABCD matrix is equal to multiplying the above matrices from left to right

$$\begin{bmatrix} 1 & 0 \\ -j\,\frac{1}{Z_1 \tan\theta_1} & 1 \end{bmatrix} * \begin{bmatrix} \cos\theta_2 & j\,Z_2\ \sin\theta_2 \\ j\,\frac{1}{Z_2}\sin\theta_2 & \cos\theta_2 \end{bmatrix} * \begin{bmatrix} 1 & 0 \\ -j\,\frac{1}{Z_1 \tan\theta_1} & 1 \end{bmatrix} =$$

$$\begin{bmatrix} \cos\theta_2 + \frac{Z_2\ \sin\theta_2}{Z_1\ \tan\theta_1} & j\,Z_2\ \sin\theta_2 \\ j\left(\frac{\sin\theta_2}{Z_2} - \frac{2\ \cos\theta_2}{Z_1\ \tan\theta_1} - \frac{Z_2\ \sin\theta_2}{Z_1^2\ \tan{\theta_1}^2}\right) & cos\,\theta_2 + \frac{Z_2\ sin\,\theta_2}{Z_1\ tan\,\theta_1} \end{bmatrix} \tag{2.12}$$

the ABCD matrix of the quarter wavelength of characteristic impedance $Z_0 = 70.7\ \Omega$ is

$$\begin{bmatrix} 0 & j\,70.7 \\ j\,0.014 & 0 \end{bmatrix} \tag{2.13}$$

the two matrices 2.12 and 2.13 should be equals and result in four equations.

$$\begin{bmatrix} \cos\theta_2 + \frac{Z_2\ \sin\theta_2}{Z_1\ \tan\theta_1} & j\,Z_2\ \sin\theta_2 \\ j\left(\frac{\sin\theta_2}{Z_2} - \frac{2\ \cos\theta_2}{Z_1\ \tan\theta_1} - \frac{Z_2\ \sin\theta_2}{Z_1^2\ \tan{\theta_1}^2}\right) & cos\,\theta_2 + \frac{Z_2\ sin\,\theta_2}{Z_1\ tan\,\theta_1} \end{bmatrix} = \begin{bmatrix} 0 & j\,70.7 \\ j\,0.014 & 0 \end{bmatrix} \tag{2.14}$$

$$cos\,\theta_2 + \frac{Z_2\ sin\,\theta_2}{Z_1\ tan\,\theta_1} = 0 \tag{2.15}$$

$$Z_2\ sin\,\theta_2 = 70.7 \tag{2.16}$$

$$\frac{sin\,\theta_2}{Z_2} - \frac{2\ cos\,\theta_2}{Z_1\ tan\,\theta_1} - \frac{Z_2\ sin\,\theta_2}{Z_1^2\ tan\,{\theta_1}^2} = 0.014 \tag{2.17}$$

$$cos\,\theta_2 + \frac{Z_2\ sin\,\theta_2}{Z_1\ tan\,\theta_1} = 0 \tag{2.18}$$

solving these four equations, the general solution is given as

$$\theta_1 = \tan^{-1}(-b), \theta_2 = \tan^{-1}(a) \tag{2.19}$$

$$Z_1 = 70.7 * \frac{\sqrt{1+a^2}}{b}, Z_2 = 70.7 * \frac{\sqrt{1+a^2}}{a} \quad (2.20)$$

where a and b are real numbers.

The design limitation is applied on the values of Z_1andZ_2, and they should be between 20 Ω and 120 Ω, and consequently the value of θ_2 is between 36 and 89 degrees. For every value of θ_2 there are many values of θ_1.

2.3 Design and Simulation

Fig. 2.6 shows the layout of the newly proposed balun, and as mentioned previous section, the three-port balun converted from the four-port network satisfies both constraints in 2.3 and 2.4 and presents a transmission stop in the even-mode circuit when its even-mode impedance approaches to zero, and achieves a good matching in the odd-mode circuit when its odd-mode impedance matches twice of the input termination impedance. The balun consists of two series transmission lines of impedance 70.7 Ω and electrical length 91°, two shunt transmission lines of impedance 49.5 Ω and electrical length 179°, and one open-ended stub of impedance 25 Ω and electrical length 91°. The three ports of the balun have impedance of 50 Ω.

By applying the LineGauge tool in the HyperLynx 3D, the lengths and widths of the transmission lines have been set and listed in Table 2.1. Fig. 2.7 shows the simulated frequency responses of the proposed balun in Fig. 2.6 with three ports terminated to 50 Ω loads. The center frequency is 2.4 GHz, the 3-dB fractional bandwidth is 40 %, the minimum insertion loss is 3 ± 0.76 dB, and the return loss is less than -10 dB over the bandwidth. Fig. 2.9 shows that the balun presents the 180 phase difference between port two and port three over the frequency range.

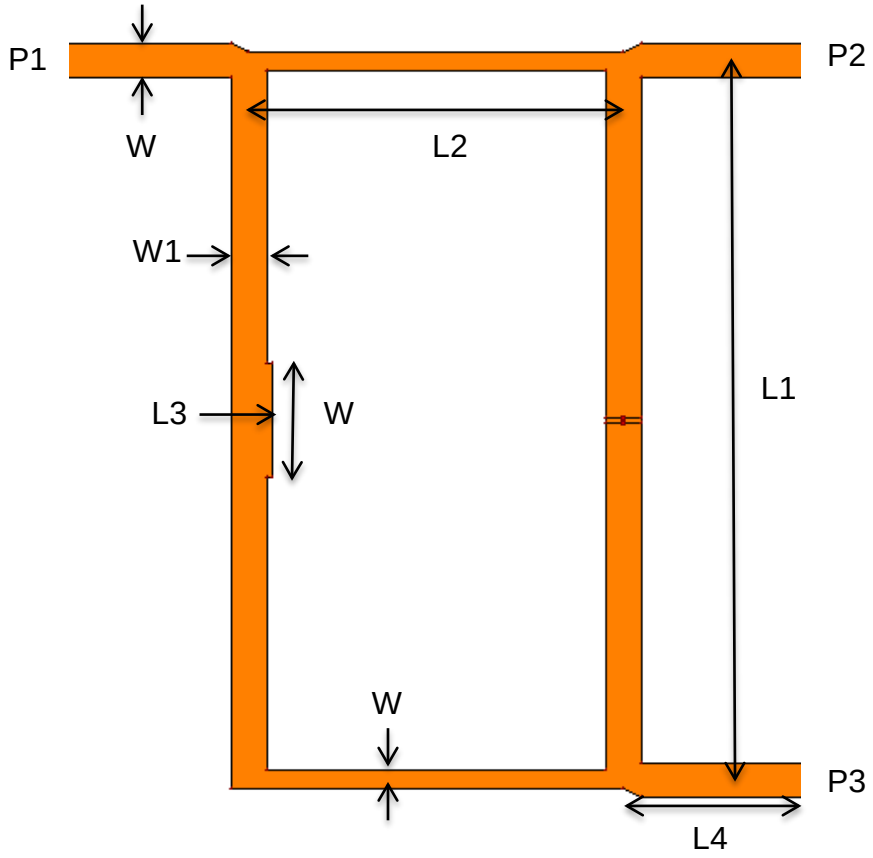

Fig. 2.6. Topology of the proposed balun.

Table 2.1

The Balun's Dimensions (Unit: Millimeter)

Length	L1	L2	L3	L4
	38	19.8	1.2	10
width	W1	W2	W3	W4
	1.9	1	4.9	1.8

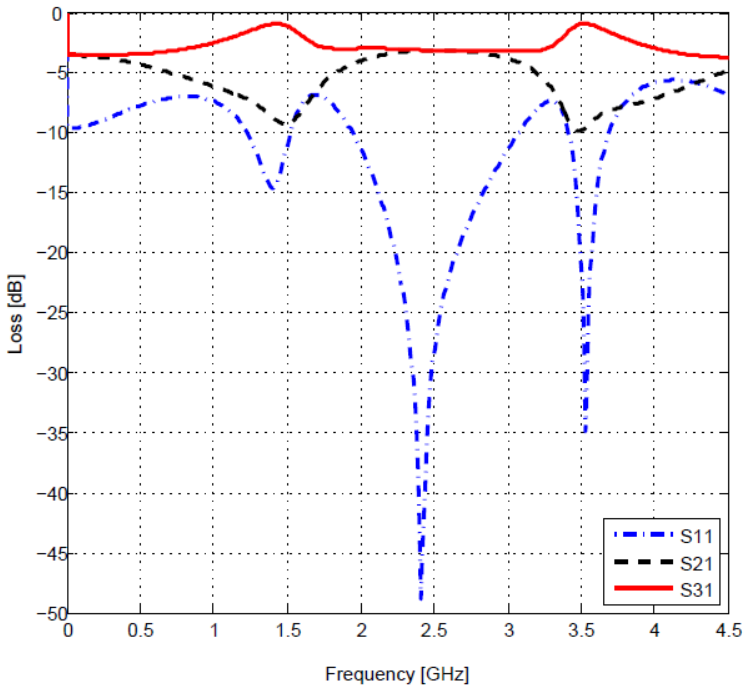

Fig. 2.7. Simulation results of return loss and insertion loss of the balun.

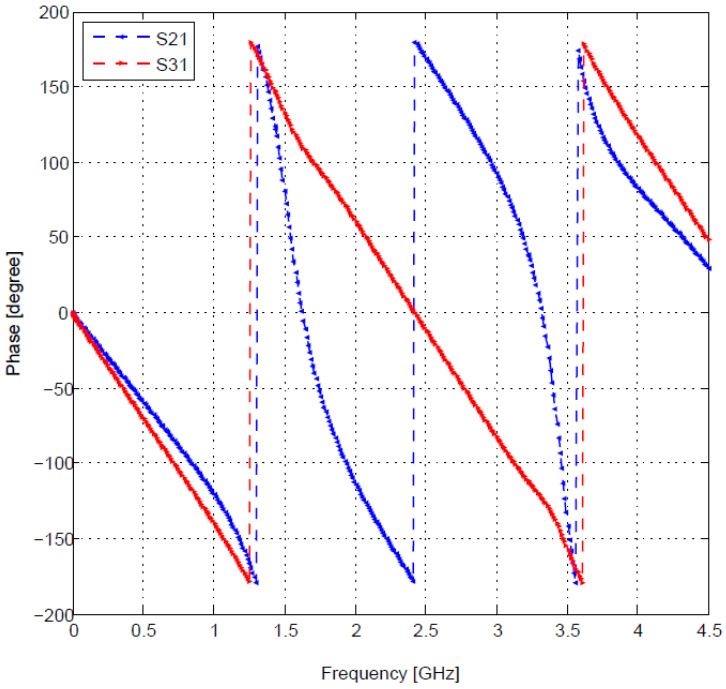

Fig. 2.8. Simulation results of phase response of the balun.

2.4 Fabrication and Measurement

To verify the design concept, the proposed balun is implemented in the microstrip structure on the RO4003 substrate (substrate thickness (h) = 0.813 mm, dielectric constant(ε_r) = 3.38, loss tangent (δ) = 0.002, and metal thickness = 17 μm). It has a circuit size of 77 mm * 39 mm. The metallization is on both sides. The top metallization consists of a microstrip feed, and the balun. The metallization on the bottom plane is a truncated microstrip ground as shown in Fig. 2.10. The measured results of return loss, insertion loss, and phase response of the balun are shown in Fig. 2.10 and Fig. 2.11 respectively. The measurements of the three-port balun are obtained by using R&S®ZVA network analyze.

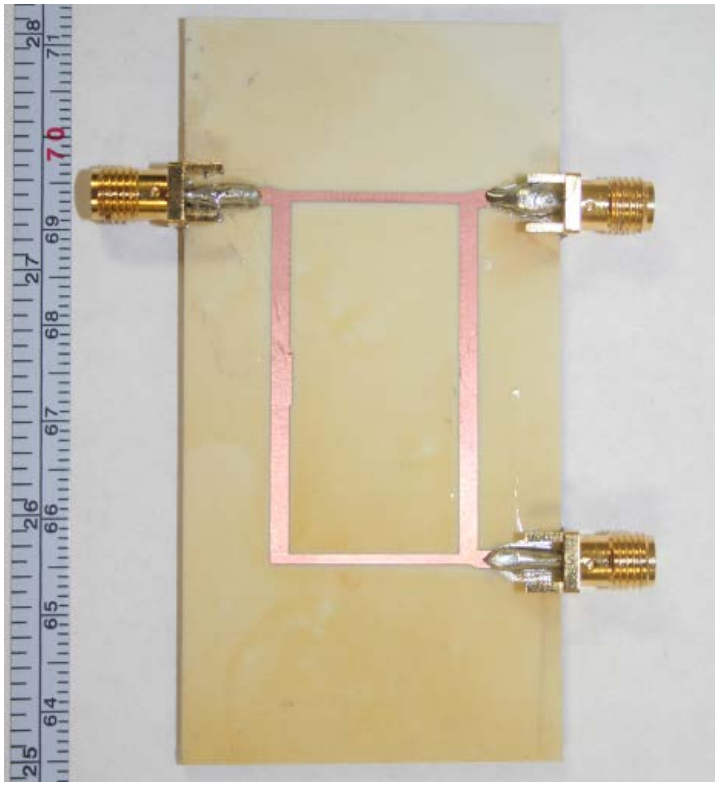

Fig. 2.9. Photograph of proposed balun.

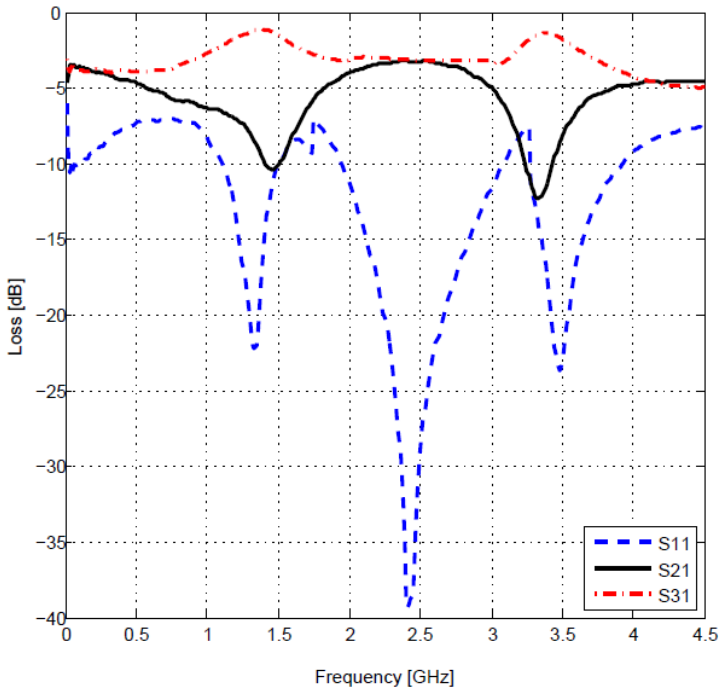

Fig. 2.10. Measurement results of return loss and insertion loss of the balun.

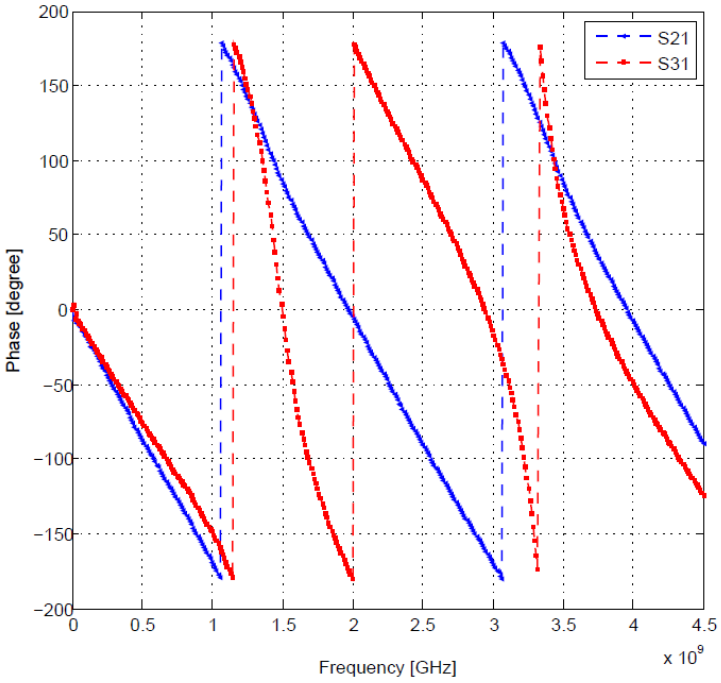

Fig. 2.11. Measurement results of phase response of the balun.

2.5 Conclusion

A new three-port balanced-to-unbalanced (balun) has been presented. The balun is employed in many wireless and microwave system, such as mixers, balanced amplifiers, and antennas. The detailed design procedures and measured results have also been discussed. This balun provides perfect balanced signals at the output ports with equal amplitudes and 180 phase difference and presents a good impedance matching at port one. The balun is designed to work at 2.4. By fabricating and measuring experimental prototypes, the performance of the proposed balun shows a very close agreement with the design concept.

CHAPTER 3

PRINCIPLE OF A QUASI YAGI ANTENNA

3.1 Introduction

A quasi Yagi antenna is a planar antenna based on conventional Yagi-Uda antenna and was first realized by Kaneda *et al* [2]. This realization adapted Yagi-Uda antenna into microwave and millimeter wave systems. Since the fundamental principles of this antenna are mostly similar to the classic Yagi-Uda antenna, Yagi-Uda antenna is presented.

3.2 Yagi-Uda Antenna

The Yagi-Uda antenna is very practical radiator working in the HF (3–30 MHz), VHF (30–300 MHz), and UHF (300–3,000 MHz) ranges [1]. It is simple to design and has a high gain. However, its bandwidth is typically small. The original design and operating fundamentals of this antenna were first presented in Japanese by S. Uda. In a later, H. Yagi described the operation of the same antenna in English.

3.2.1 Structure of Yaqi-Uda Antenna

The general configuration of Yagi-Uda antenna is shown in Figure 3.1. The antenna is mainly an array of linear dipole elements with one element serving as the driven excited directly by a feeding transmission line while the others act as parasitic elements [1]. The parasitic elements are excited through mutual coupling between adjacent elements. As shown in Figure 3.1, the Yagi-Uda antenna consists of three parts. The first part is the longest element located at the left side of the driven element.

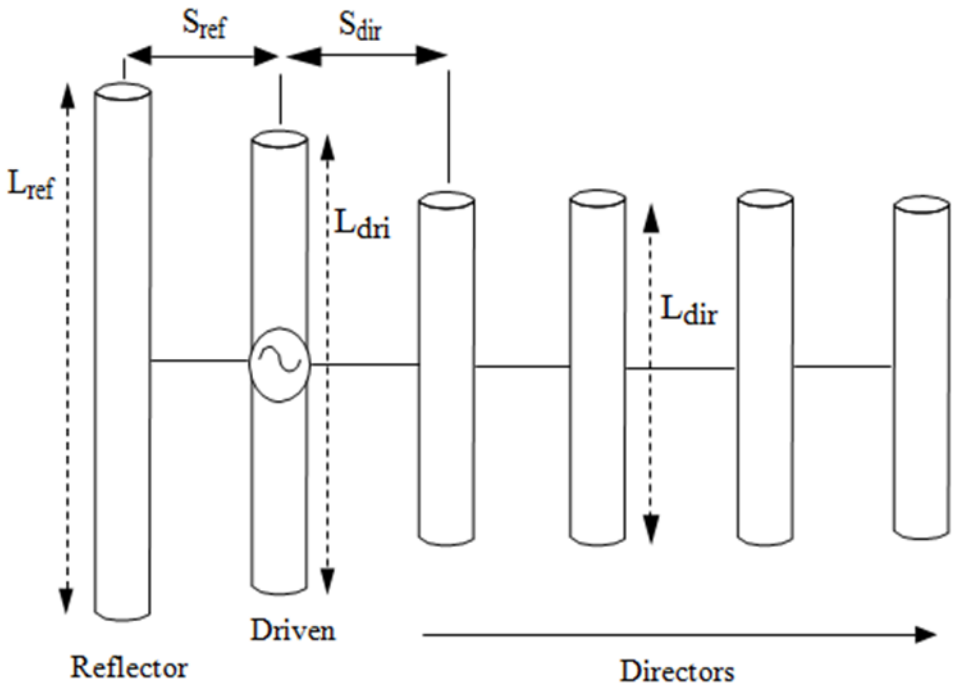

Fig. 3.1. Yaqi-Uda antenna

The length of this element is given as L_{ref}, and the space between the driven and this element is S_{ref}. This element is named a reflector because it has an important effect on the front-to-back ratio of the antenna, that is, the reflector is longer than its resonant length. As a result, the impedance of the reflector will be inductive, and consequently the phase of the currents flowing in the reflector will lag the voltage induced on the reflector, and this will improve the front-to-back ratio and the directivity of Yagi-Uda antenna. The second part is the driven element, and its length is given as L_{dir}. It is simply a half-wave dipole and the only element in the structure fed by a transmission line at its center, and the other elements are parasitic which reflect or steer the energy in a particular direction. When incident waves are applied to the driven element, induced currents will be created on the surface of the driven. The currents are decreasing in the magnitude toward the end of dipole until they become zero at the dipole terminals which build up electrical charges of opposite signs on each dipole's end, that is, the term

"dipole" comes from charges accumulation on both terminals. The driven element affects the input impedance of the antenna and also the front-to-back ratio. The third part is the shortest element to the right of the driven. The element is of length L_{dir} and separated from the driven by a distance S_{dir}. It is known as a director. There can be any number of directors. The directors have large effect on the gain of the antenna and the wave propagation in a particular direction.

3.2.2 End-Fire Radiation of Yagi-Uda Antenna

Because of the arrangement of this antenna, it exclusively operates as an end-fire array, and it is achieved by having the parasitic elements in the forward beam act as directors while those in the rear act as reflectors. The end-fire beam pattern occurs when the parasitic elements in the direction of the beam are somewhat smaller in length than the driven element. Typically the driven element length is between 0.45λ and 0.49λ whereas the length of the directors should be about 0.4λ to 0.45λ. However, the directors may not necessarily have the same length. The distance between the directors is typically 0.3λ to 0.4λ, and that is not necessarily for optimum designs. It has been shown experimentally that for a Yagi-Uda array of 6λ total length the overall gain was independent of director spacing up to about 0.3λ. However, for a director spacing greater than 0.3λ, a significant drop in the gain was noticed [1]. This loss refers to a rapid drop in the magnitude of the currents between the driven element and the director. The length of the reflector is somewhat greater than that of the driven dipole. In addition, the separation between the driven element and the reflector is somewhat smaller than the spacing between the driven element and the nearest director, and it is

found to be near 0.25λ [1]. As discussed in section 3.2.1, Since the length of the reflector is greater than its resonant length, the impedance of the reflector is inductive, and its current lags the induced voltage. Differently, the length of the director is smallar than its resonant length which means the impedance of the director is capacitive, and its current lead the induced voltage.

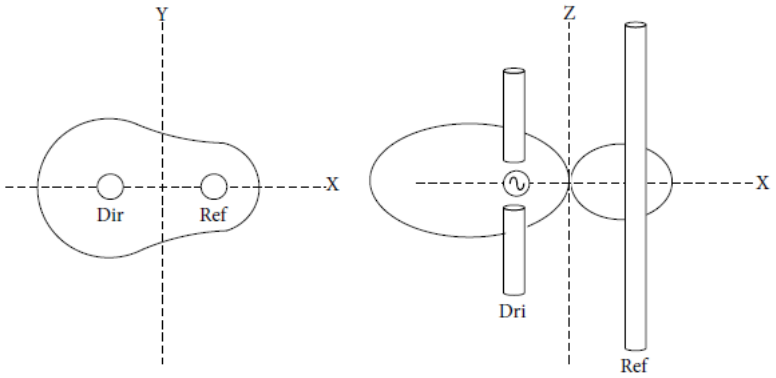

(a)

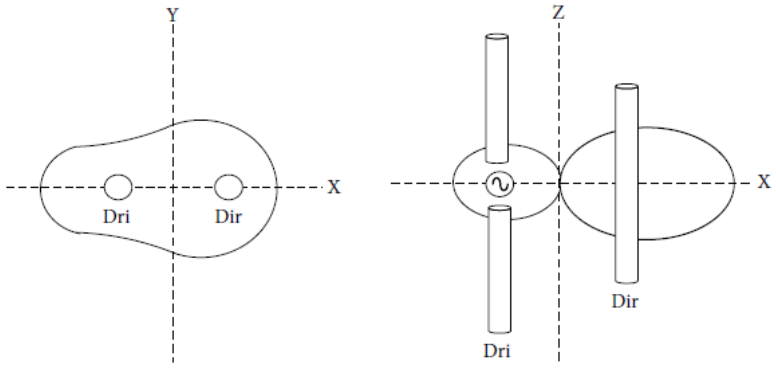

(b)

Fig. 3.2. End-fire beam of Yagi-Uda antenna. (a) Driven with parasitic element acts as a reflector. (b) Driven with parasitic element acts as a director.

These chosen lengths along with spacing between antenna elements will form an array with currents approximately equal in magnitude and with equal progressive phase shifts which will reinforce the field of the driven element toward the director. Thus, Yagi-

Uda antenna may be regarded as a structure supporting a traveling wave whose performance is determined by the current distribution in each element and the phase velocity of the traveling wave [1]. Figure 3.2 illustrates a directional pattern formed by this configuration of Yagi-Uda antenna [3].

The forward and backward gain, input impedance, bandwidth, front to back ratio, and magnitude of minor lobes are the most radiation characteristics of interest for Yagi-Uda antenna. These characteristics can be improved by optimizing parameters, such as the lengths and diameters of reflectors and directors, as well as their respective spacing. There is a trade-off between radiation characteristics of the antenna. For instant, increasing the input impedance and expanding the bandwidth of the antenna can be achieved at expense of other parameters, such as the gain and the magnitude of minor lobes. However, using a two-element folded dipole with a step-up ratio as a driven can increase the input impedance of the antenna without affecting the performance of other parameters.

3.2.3 Yagi-Uda Antenna as an End-Fire Array

Another way to increase the dimensions of the antenna, that leads to more directive characteristics and without enlarge the size of the individual elements, is to arrange the antenna elements in such an electrical and geometrical configuration. This configuration is referred to as an array. The radiation between the elements of that array adds up to enhance the radiation in a particular direction and reduce it in the other directions.

Theoretically the total amount of field radiated by the array is equal to the vector summation of the fields radiated by individual elements, but practically there are at least five parameters that are used to shape the overall pattern of the array of identical elements [1].

1. The geometric shapes of the array (circular, linear, etc.)
2. The spacing between adjacent elements
3. The excitation amplitude of the individual elements
4. The excitation phase of the individual elements
5. The relative pattern of the individual elements

An array of two infinitesimal horizontal dipoles, as shown in Figure 3.3(a), the total field radiated with neglecting the coupling between the adjacent elements is given by

$$E_t = E_1 + E_2 = \widehat{a_\theta} j\eta \frac{KI_0 l}{4\pi} \left\{ \frac{e^{-j\left[kr_1 - \left(\beta/2\right)\right]}}{r_1} \cos\theta_1 + \frac{e^{-j\left[kr_2 - \left(\beta/2\right)\right]}}{r_2} cos\,\theta_2 \right\} \qquad (3.1)$$

As illustrated in Figure 3.3(b), and at the observation point in far-field region, the phase and amplitude variations are given by

$$\left.\begin{aligned} r_1 &= r - \frac{d}{2}\cos\theta \\ r_2 &= r + \frac{d}{2} cos\,\theta \end{aligned}\right\} \text{ for phase variations} \qquad (3.2)$$

$$r_1 \approx r_2 \approx r \qquad \text{for amplitude variations} \qquad (3.3)$$

This assumption reduces the equation (3.1) to

$$E_t = \widehat{a_\theta} j\eta \frac{KI_0 l e^{-jkr}}{4\pi r} \cos\left\{2\ \cos\left[\frac{1}{2}\ (kd\ \cos\theta + \beta)\right]\right\} \qquad (3.4)$$

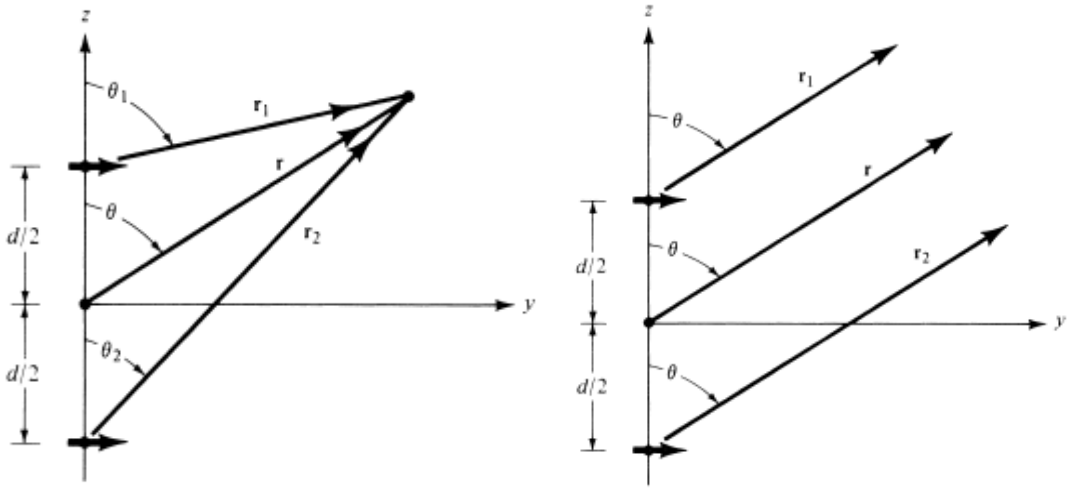

(a) Two infinitesimal dipoles (b) Far-field observations

Fig. 3.3. Geometry of two-element array along Z-axis.

From equation (3.4) it is obvious that the total field radaited from the two-element array is equal to the field ratiated from a single element located at the origin multiplied by a factor referred as the array factor, and it is given by

$$\mathrm{AF} = 2\ cos\left[\frac{1}{2}\ (kd\ cos\theta + \beta)\right] \tag{3.5}$$

and after it is normalized, it can be written as

$$\mathrm{AF} = cos\left[\frac{1}{2}\ (kd\ cos\theta + \beta)\right] \tag{3.6}$$

The field in the far-zone of an identical two-element array is equal to the product of the field of a single element, at a selected reference point (usually the origin), and the array factor of that array. That is,

$$\mathrm{E(total)} = [\mathrm{E(single\ element\ at\ reference\ point)}] \times [\mathrm{array\ factor}] \tag{3.7}$$

The number of antenna elements, how these elements are arranged, the space between the elements, and their relative phases and magnitudes control the array factor

To illustrate how the array factor affects the total pattern of the antenna array, the pattern of single element, the array factor, and the total pattern of the arra are shown in Figure 3.4. Due to the array factor, the null is at $\theta = 90^{\circ}$ in the total pattern. The phase difference is 90 degree ($\beta = 90^{\circ}$).

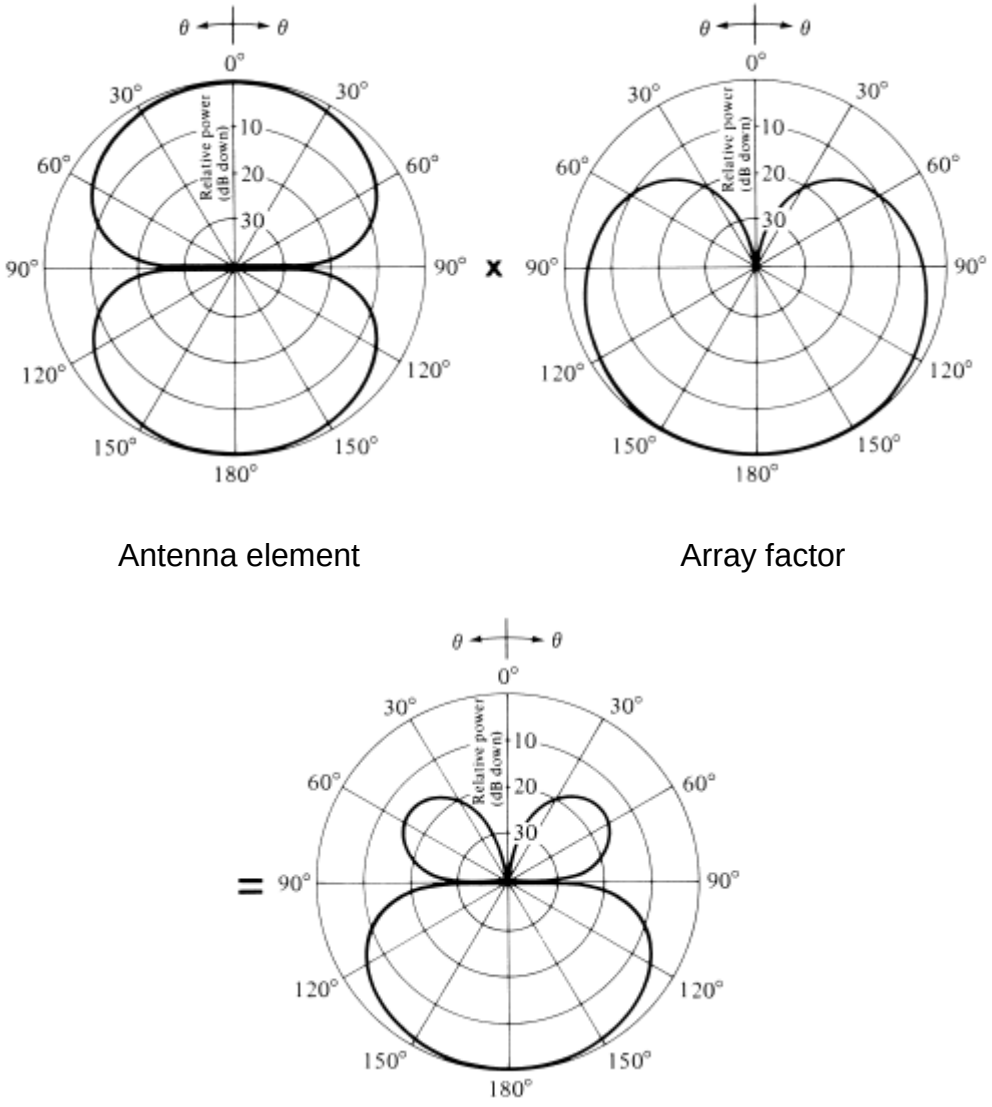

Antenna element Array factor

Total pattern

Fig. 3.4. The pattern of antenna element, array factor, and total array pattern after pattern multiplication.

For the *N*-element linear antenna array with uniform amplitude and spacing, the final array factor (AF) can be written as

$$\mathrm{AF} = 1 + e^{j(kd\cos\theta+\beta)} + e^{j2(kd\cos\theta+\beta)} + \cdots + e^{j(N-1)(kd\cos\theta+\beta)}$$

$$\mathrm{AF} = \sum_{n=1}^{N} e^{j(n-1)(kd\cos\theta+\beta)}, \quad k = \frac{2\pi}{\lambda} \tag{3.2}$$

Here, λ is the wavelength of the signal, d and β is the distance and phase difference between two adjacent antenna elements respectively, θ presents the direction of the radiation beam. Finally, the above equation can be summarized to

$$\mathrm{AF} = \sum_{n=1}^{N} e^{j(n-1)\psi}, \ \ \psi = kd\cos\theta + \beta \tag{3.3}$$

as indicated in equation (3.3), the total array factor is a sum of exponentials, and it could be described as the vector summation of N phasors each of them is unit amplitude with ψ as a progressive phase. This is shown by the phasor diagram in Figure 3.5. It is clear from the phasor diagram that a selected phase difference ψ between the array elements can dominate the array factor for a uniform array. However, in a nonuniform array, both the amplitude and the phase can be used to control the total array factor. After some calculations, the array factor in equation 2.3 can be simplified into a compact form.

$$\mathrm{AF} = \left[\frac{\sin\left(\frac{N}{2}\psi\right)}{\sin\left(\frac{1}{2}\psi\right)}\right] \tag{3.4}$$

For small values of ψ, the equation 2.4 can be roughly written as

$$\mathrm{AF} \approx \left[\frac{\sin\left(\frac{N}{2}\psi\right)}{\frac{\psi}{2}}\right] \tag{3.5}$$

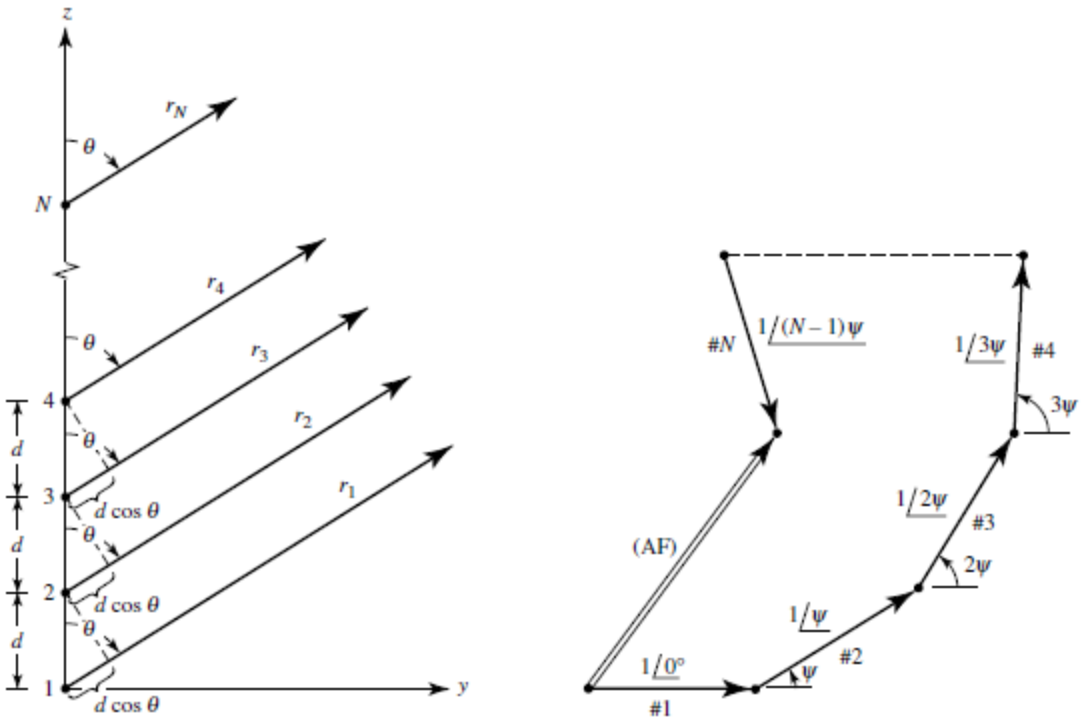

(a) (b)

Fig. 3.5. (a) Far-field geometry and (b) phasor diagram of *N*-element array.

3.3 Conclusion

The performance of a Yagi-Uda antenna is controlled the lengths of the elements and the distances between them. The front-to-back ratio is affected by the reflector and the driven dipole. However, the driven dipole has large impact on the input impedance of the antenna. The length and spacing of the director have significant effect on the forward gain and input impedance matching.

CHAPTER 4

A PLANAR QUASI-YAGI ANTENNA FED BY THE PROPOSED BALUN

4.1 Introduction

The concept of the quasi-Yagi antenna comes from the conventional Yagi-Uda antenna to adapt it into the microwave and millimeter wave systems. The quiz-Yagi antenna has compact size, low-profile, lightweight, low-cost, and compatibility with microwave circuits and was first presented in [2]. It basically consists of a balanced-to-unbalanced (balun) feeding structure, a driven dipole, a parasitic director, and a truncated ground plane acts as a reflector. Since the antenna is a balanced structure, whereas the feeder is usually an unbalanced transmission line, the balun feeding network is necessary for the antenna to convert the unbalanced signal at the input to the balanced signal at the output. Due to the necessity of the balun, most of the recent research about the quasi-Yagi antenna focuses on designing the baluns [16]-[20].

In [16], a four-port bandpass filter is converted into a three-port balun to feed a quasi-Yagi antenna. An integrated balun of stepped impedance coupled structure is employed to feed an ultra-wideband quasi-Yagi antenna in [17]. A coplanar waveguide (CPW) fed a quasi-Yagi antenna has been demonstrated in [18]. In [19], two parallel strips on two substrate layers with truncated ground plane is presented as feeding structure for quasi-Yagi antenna. In [20], a uniplanar coplanar waveguide fed quasi-Yagi antenna is proposed. The drawback of the quasi-Yagi antenna introduced in [16] is that the antenna is built in the three-metal-layer structure that introduces design complexity, and the antenna becomes incompatible with the microwave integrated circuits. In this chapter a planar quasi-Yagi antenna reported in [16] fed by the proposed balun is

introduced, and the simulated and measured performance of the uniplanar antenna indicate less than –10 dB return loss and 3.9–4.3 dBi gain across 36 % fractional bandwidth centered at 2.8 GHz.

4.2 Design and Simulation

Fig. 4.1 shows the uniplanar quasi-Yagi antenna. The wideband balun bandpass filter presented in [16] is replaced by the proposed planar microstrip balun. Since the director element is excited parasitically by induced current in the driven element, the distance between the two elements (S_{dir}) is chosen to be less than a quarter-wavelength.

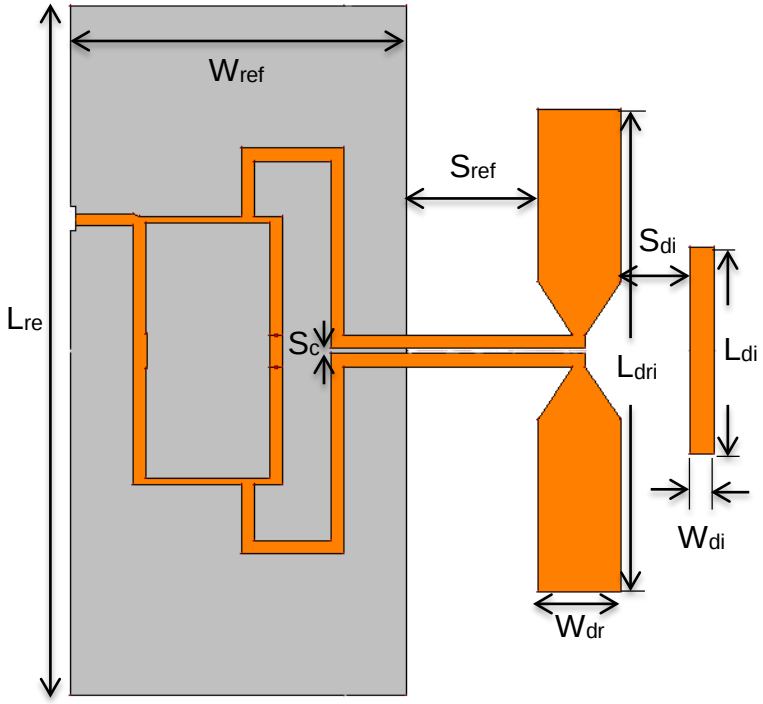

Fig. 4.1. Layout of the quasi-Yagi antenna utilizing the proposed balun.

The spacing (S_{ref}) between the driven dipole and the reflector which is here the truncated ground plane should be equal to a quarter-wavelength to create an in-phase reflected wave along the end-fire direction [16]. Increasing the wave traveling along the

end-fire direction will enhance the antenna directivity. One of the most unique and effective features of this antenna is the use of the truncated ground plane as the reflector element. The driven printed dipole is used to generate a TE_0 surface wave with very little undesired TM_0 content [21]. As with the classic Yagi-Uda antenna, a proper design of the quasi-Yagi antenna requires careful optimization of the driven, director, and reflector (ground plane) parameters, which include element spacing, length, and width. The antenna's dimensions are list in Table 4.1.

Table 4.1

The Quasi-Yagi Antenna's Dimensions (Unit: Millimeter)

Length	L_{dir}	L_{dri}	L_{ref}
	30	70	100
width	W_{dir}	W_{dri}	W_{ref}
	3.6	12	48.7
Spacing	S_{dir}	S_{cps}	S_{ref}
	10	0.8	19

The integrated quasi-Yagi antenna has been designed and simulated. Fig. 4.2 shows the simulated return loss with better than -10 dB from 2.3 to 3.34 GHz, indicating that a fractional bandwidth of 36% can be obtained for this antenna.

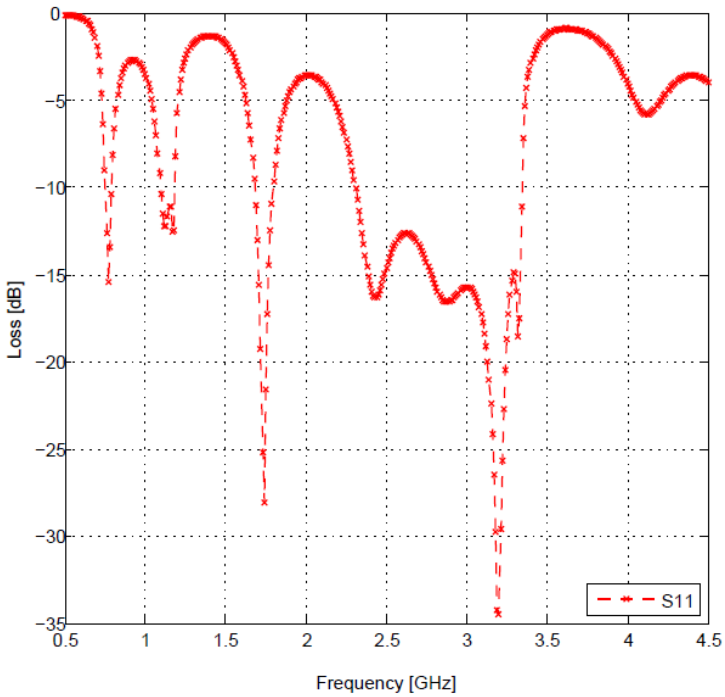

Fig. 4.2. Simulated return loss of the planar quasi-Yagi antenna.

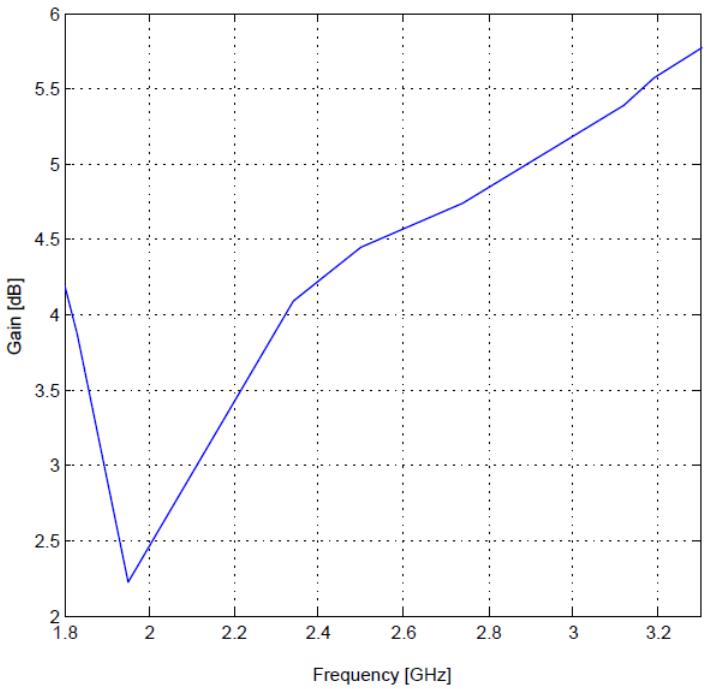

Fig. 4.3. Simulated gain of the planar quasi-Yagi antenna.

Fig. 4.3 also illustrates the simulated antenna gain, and it is approximately 3.9–4.3 dBi.

Fig. 4.4 shows the E-plane and H-plane radiation pattern of the antenna.

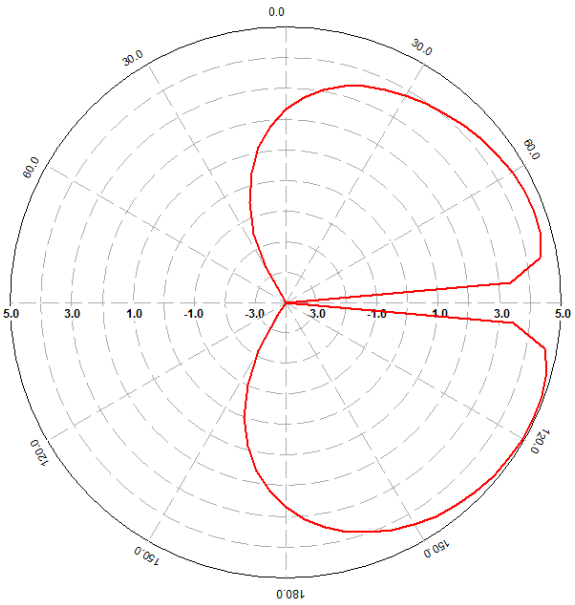

(a)

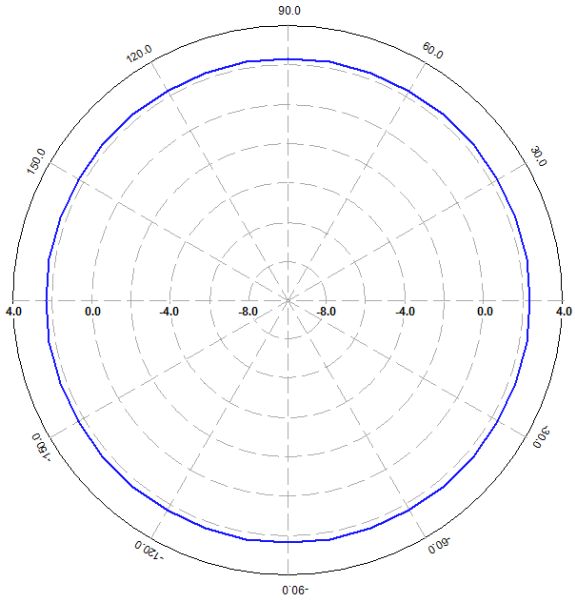

(b)

Fig. 4.4. (a) The E-plane and (b) H-plane radiation pattern of the antenna.

4.3 Fabrication and Measurements

To further illustrate the performance of the proposed balun, it is realized and used to feed the quasi-Yagi antenna in [16]. The realized balun provides good output

balanced signals and maintains a well- defined return-loss response throughout the operating bandwidth. The quasi-Yagi antenna is implemented in the microstrip structure on the RO4003 substrate (substrate thickness(h) = 0.813 mm, dielectric constant(ε_r) = 3.38, loss tangent (δ) = 0.002, and metal thickness = 17 μm). It has a circuit size of 134 mm * 115 mm.

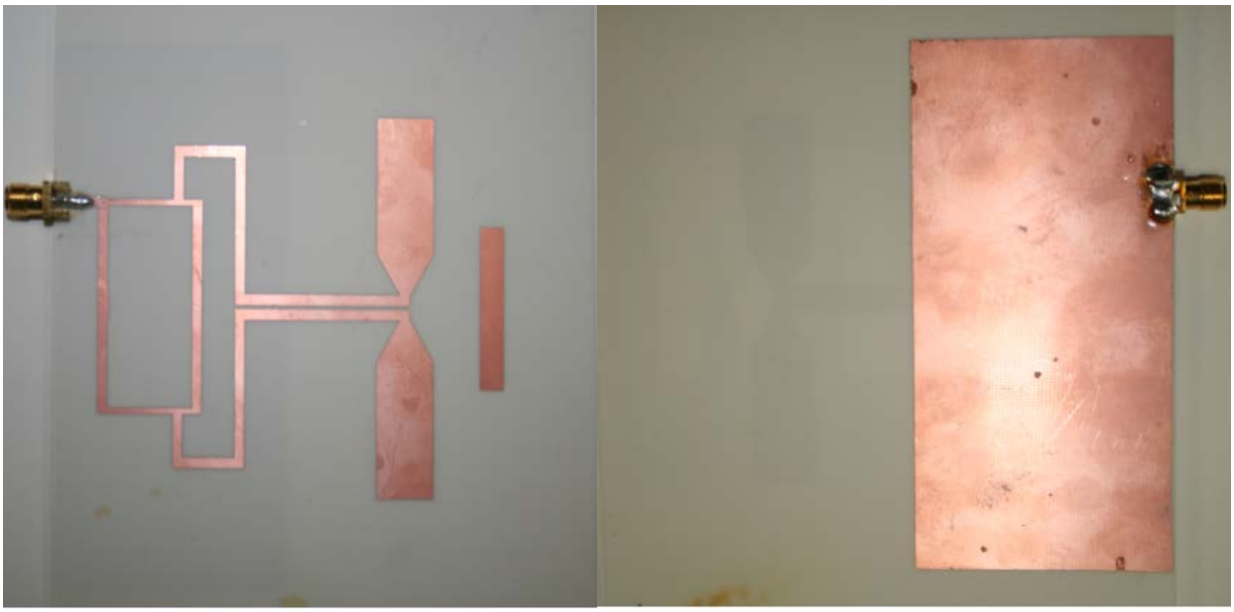

(a) (b)

Fig. 4.5. (a) Top side and (b) bottom side of the fabricated quasi-Yagi antenna.

Fig. 4.5 shows the physical layout of the implemented quasi-Yagi antenna. The truncated ground plane is located under the feeding structure (balun). Shown in Fig. 4.6 is the measured results for the return loss. A good agreement between them and the simulated results in Fig. 4.2 is observed. The measured return loss is better than 10 dB from 2.3 to 3.3 GHz, indicating that a bandwidth of 36% can be obtained for the antenna.

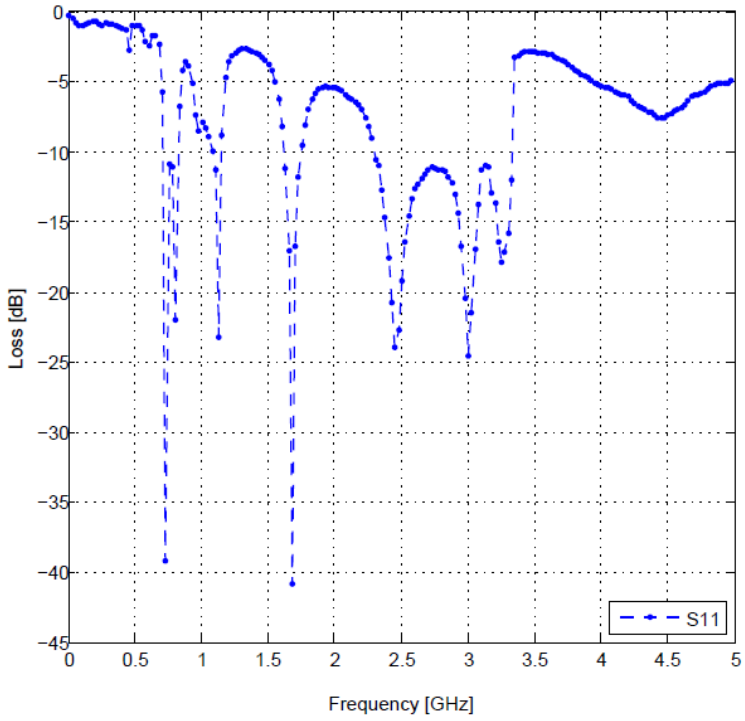

Fig. 4.6. Measured return losses of the quasi-Yagi antenna.

4.4 Impact of Director on Quasi-Yagi Antenna's Performance

The parasitic director element in front of the driven dipole directs the antenna propagation toward the end-fire direction, enhances the gain and front-to-back ratio of the antenna, and acts as an impedance-matching parasitic element with driven element. In this section, the quasi-Yagi antenna (Fig. 4.7) is simulated and measured without the director, and the results are compared with the antenna in Fig. 4.5.

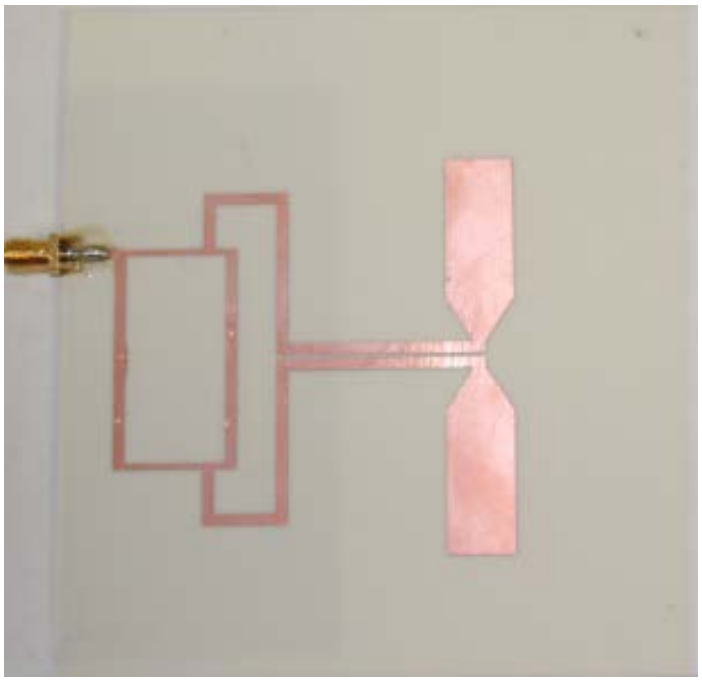

Fig. 4.7. Quasi-Yagi antenna without parasitic director element.

The results for return loss are shown in Fig. 4.8 and 4.9. The director affects the bandwidth to be reduced by more than 50%. A very close agreement between simulated and measured results is. This may refer to impedance-mismatching between the input and output of the antenna since the director acts as an impedance-matching parasitic element. In Fig. 4.10, the simulated antenna gain is shown. The gain of the antenna without director is decreased in comparison with the antenna gain with the director since this parasitic element has large impact on the end-fire radiation pattern of the antenna. E-plane and H-plane radiation patterns are illustrated in Fig. 4.11 and 4.12 respectively. As the antenna gain is affected by director, also the radiation pattern will be affected.

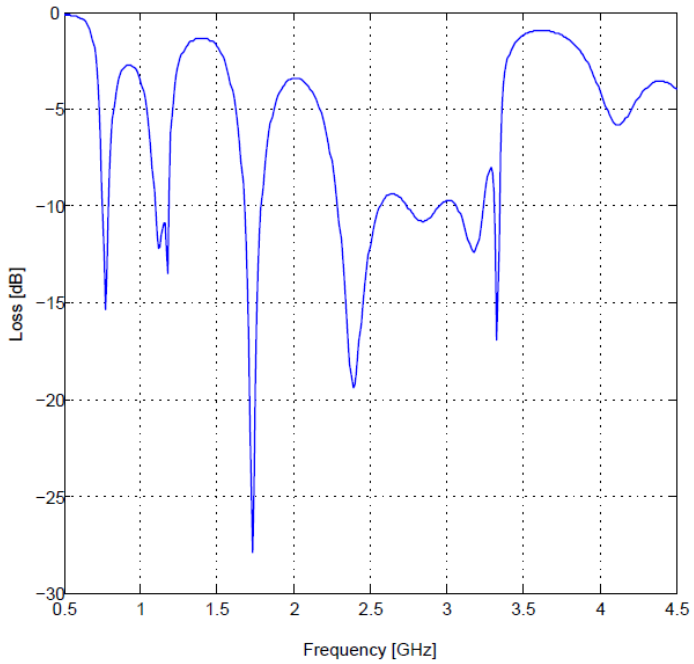

Fig. 4.8. Simulated return losses of the quasi-Yagi antenna without director.

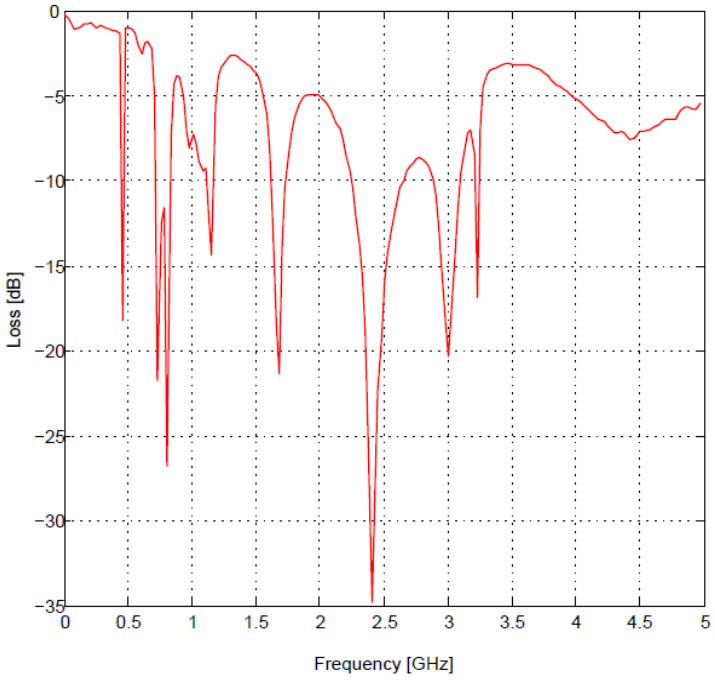

Fig. 4.9. Measured return losses of the quasi-Yagi antenna without director.

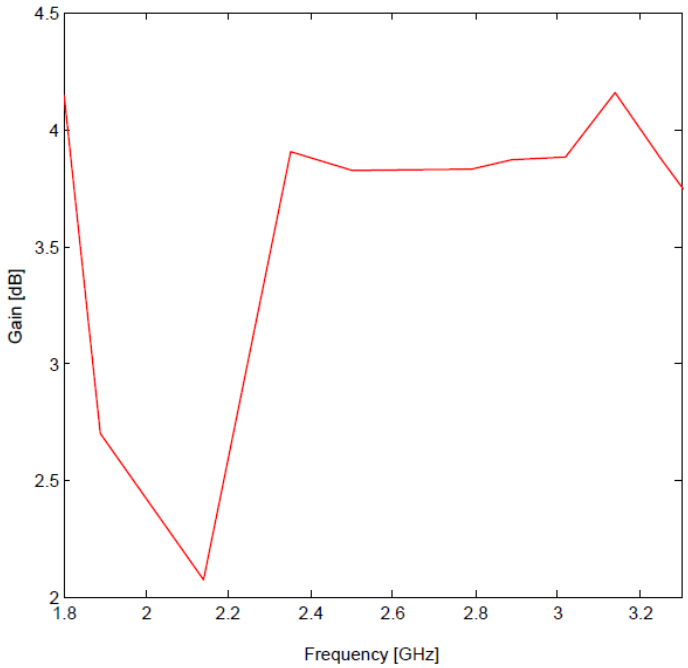

Fig. 4.10. Simulated gain of the quasi-Yagi antenna without director.

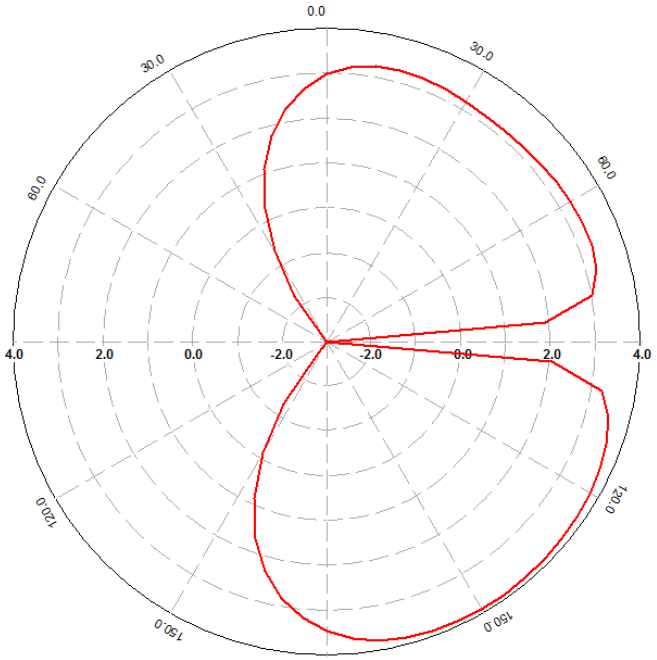

Fig. 4.11. The E-plane radiation pattern of the antenna without director.

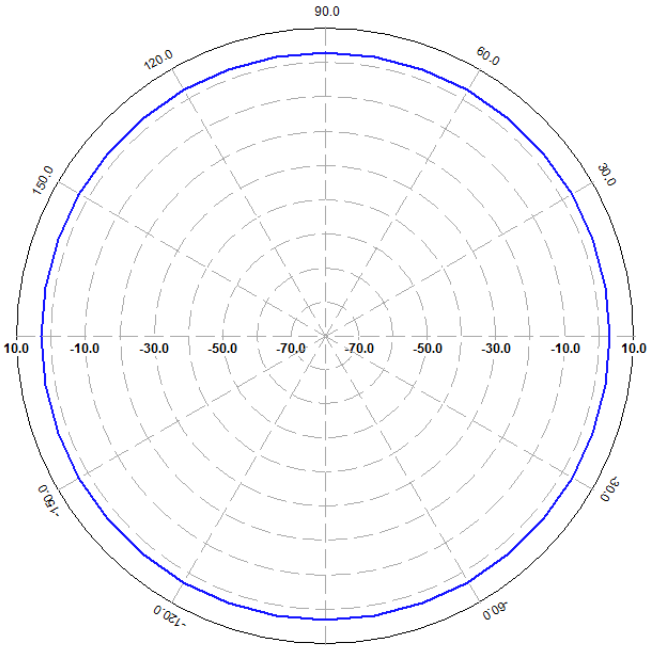

Fig. 4.12. The H-plane radiation pattern of the antenna without director.

4.5 Conclusion

This chapter has demonstrated a uniplanar quasi-Yagi antenna. To realize the function of the proposed balun, the balun is integrated with a quasi-Yagi antenna. The balun as a feeding network for the antenna presents a good performance and expected achievement. The antenna is fabricated on a single substrate (RO4003) with metallization on both sides. The bottom side is a truncated ground plane located under the feeding network, and it serves as a reflector element for the antenna. The top side consists of the proposed balun and two dipole elements, one of which is the driven element fed by the proposed balun and the second dipole is the parasitic director. The antenna has been simulated and tested. The measured results are in close agreement with the simulated results. The director effect on the antenna's performance is introduced and verified. The results show that the input impedance and the gain of the antenna have been affected by the absence of the parasitic director. The simulated and

measured results of the return loss and the gain agree well, demonstrating a significant reduction in the antenna’s performance.

CHAPTER 5

CONCLUSION AND FUTURE WORK

5.1 Conclusion

In this thesis, a novel approach about the design and the implementation of planar balun is presented. A proposed balun (working at 2.4 GHz) is designed, fabricated, and tested. The proposed balun features compact size, low profile, and large design flexibility. The proposed balun demonstrates a perfect balanced output with equal amplitude and 180 phase difference and good input matching with 50% fractional bandwidth better than -10 dB. These results demonstrate that this new balun is highly suited for wireless communication applications. Such balun is used to feed a quasi-Yagi antenna. This antenna is designed and fabricated and achieves a measured 36% frequency bandwidth for return loss less than -10 dB. The impact of the parasitic director is also investigated. The antenna faced a reduction in both the bandwidth and gain without this element.

5.2 Future Work

In the future, in order to further improve the performance of balun, more different designs featuring characteristics such as compact size, wide bandwidth, and low cost productions need to be investigated. The approach used to design this balun introduces many design parameters that can further improve the balun's performance.

REFERENCES

[1] C.A Balanis, “Antenna Theory Analysis and Design,” John Wiley & Sons, INC. 3rd

Edition, New York, 2005, pp.577-580.

[2] N. Kaneda, Y. Qian, and T. Itoh, “A novel Yagi-Uda dipole array fed by a microstrip-to-CPS transition,” in *Asia-Pacific Microwave Conf. Deg.,* Yokohama, Japan, pp. 1413-1416, Dec. 1998.

[3] http://www.antenna-theory.com/antennas/travelling/yagi.php.

[4] J. J. Yao, C. Lee, and S. P. Yeo, “Microstrip branch-line couplers for crossover application,” *IEEE Trans. Microw. Theory & Tech.,* vol. 59, no. 1, pp. 87- 92, Jan. 2011.

[5] B Mayer and R Knoechel, “Biasable balanced mixers and frequency doublers using a new planar balun,” *Conference Proceeding: 20th European Microwave Conference,* V2, pp. 1027-1032, 1990.

[6] R. Sturdivant, “Balun design for wirless, mixers amplifiers, and antennas,” *Appl. Microwaves*, vol. 5, pp. 34-44, Summer 1993.

[7] D. Raicu, “Design of planar, single-layer microwave baluns,” in *IEEE MTT-S Int. Microwave symp. Dig*, pp. 801-804, 1998.

[8] B. Climer, “Analysis of suspended microstrip taper baluns,” *Proc. IEE*, Vol. 135, Pt H, No. 2, pp. 65-69, April 1988.

[9] A. M. Pavio and A. Kikel, “A monolithic or hybrid broadband compensated balun,” in *IEEE MTT-S Int. Microwave symp. Dig*, pp. 483-486, 1990.

[10] Y. C. Leong, K. S. Ang, and C. H. Lee, “A derivation of a class of 3-port baluns from symmetrical 4-port networks,” *IEEE MTT-S Digest*, pp. 1165-1168, 2002.

[11] H. K. Chiou, H. H. Lin, and C. Y. Chang, “Lumped-element compensated high/low-pass balun design for MMIC double-balanced mixer”, *IEEE Microwave Guided Wave Lett.*, vol. 7, pp. 248-250, Aug. 1997.

[12] Samuel J. Parisi, “Monolithic, lumped element, single sideband modulator,” *IEEE MTT-S International Microwave Symp. Dig.,* pp. 1047-1050, 1992.

[13] K. S. Ang, Y. C. Leong, and C. H. Lee, “Analysis and design of miniaturized lumped-distributed impedance-transforming baluns,” *IEEE Transactions on Microwave Theory and Techniques,* vol. 51, no. 3, March 2003.

[14] C. W. Tang and C. Y. Chang, “A semi-lumped balun fabricated by low temperature co-fired ceramic,” in *IEEE MTT-S Int. Microwave Symp. Dig.*, pp. 2201–2204, 2002.

[15] B. P. Kumar, G. R. Branner, and B. Huang, “Parametric analysis of improved planar balun circuits for wireless microwave and RF applications,” in *Proc. IEEE Midwest Circuits and Systems Symp.*, pp. 474–475, 1998.

[16] C. H. Wu, C. H. Wang, S. Y. Chen, and C. H. Chen, “Balanced-to-unbalanced bandpass filters and the antenna application,” *IEEE Trans. Microw. Theory and Tech.*, vol. 56, no. 11, pp. 2474–24826, Nov. 2008.

[17] A. Abbosh, “Ultra-wideband quasi-Yagi antenna using dual-resonant driver and integrated balun of stepped impedance coupled structure,” *IEEE Transactions on Antennas and Propagation*, vol. 61, no. 7, pp. 3885-3888, Jul. 2013.

[18] J. Sor, Y. Qian, and T. Itoh, “Coplanar waveguide fed quasi-Yagi antenna,” *Electron. Lett.*, vol. 36, no. 1, pp. 1–2, 2000.

[19] G. Zheng, A. Kishk, A. Glisson, and A. Yakovlev, “Simplified feed for modified printed Yagi antenna,” *Electron. Lett.*, vol. 40, no. 8, pp. 464–466, 2004.

[20] H. Kan, A. Abbosh, R. Waterhouse, and M. Bialkowski, “Compact broadband coplanar waveguide-fed curved quasi-Yagi antenna,” *IET Microw. Antennas Propag.*, vol. 1, no. 3, pp. 572–574, 2007.

[21] N. G. Alexopoulos, P. B. Ketehi, and D. B. Rutledge, “Substrate optimization for integrated circuit antennas,” *IEEE Trans. Microwave Theory Tech.*, vol. MTT-31, pp. 550–557, July 1983.